



Fire induced concrete spalling in combination with size effects

André Klimek · Ludwig Stelzner · Sascha Hothan · Andreas Rogge

Received: 19 April 2022 / Accepted: 18 September 2022
© The Author(s) 2022

Abstract The size effect has its origin in fracture mechanics and describes the formation as well as propagation of cracks in brittle and solid materials in dependence of the specimen size. However, the size effect in concrete spalling describes the damage behaviour on a macroscopic scale for different sized specimens in case of fire. Concrete spalling is a very complex and yet not fully understood phenomenon. To reduce the effort of fire tests to analyse the spalling behaviour of concrete mixtures, this study investigates the susceptibility to spalling for six different concrete mixtures and three specimen sizes. The sizes were divided in full scale slabs (1.8 m × 1.2 m × 0.3 m), intermediate scale cuboids (0.6 m × 0.6 m × 0.3 m) and small scale cylinders (Ø0.15 m × 0.3 m). For this purpose, a novel test set-up was built to test six intermediate scale or twelve small scale specimens simultaneously to ensure a similar heating regime for every specimen. All specimens were fire exposed on one side and remained unrestrained. A size effect

occurred for four of the six concrete mixtures. Compared to the full scale specimens the spalling was reduced significantly for all smaller specimen sizes. Additionally, spalling did not occur for the small scale specimens. The results show that the specimen size is an essential parameter to investigate the susceptibility to spalling of a concrete mixture. For future investigations the testing conditions must be adjusted for the intermediate scale specimens to recreate the conditions of the slabs.

Keywords Concrete · Spalling · Size effect · Fire test

1 Introduction

Ordinary concrete (OC) is a fundamental and versatile material in the building construction industry and one of the most common material in civil engineering. Specifications of applications require an adjustment of concrete mixtures. Considering high performance concretes (HPC) the application of high strength concrete (HSC) enables a reduction of the cross-section area maintaining a high load bearing capacity, whereas self-compacting concrete mixtures (SCC) show a good workability. Furthermore, complex environments have special demands on concrete members e.g. tunnel linings. All these concrete

A. Klimek (✉) · L. Stelzner · S. Hothan · A. Rogge
Bundesanstalt für Materialforschung und -prüfung, Unter
den Eichen 87, 12205 Berlin, Germany
e-mail: andre.klimek@bam.de

L. Stelzner
e-mail: ludwig.stelzner@bam.de

S. Hothan
e-mail: sascha.hothan@bam.de

A. Rogge
e-mail: andreas.rogge@bam.de



mixtures are prone for spalling in case of fire [1–4]. Spalling leads to an increase of the concrete temperature in deeper parts of the member. Reinforcement bars can be exposed to high temperatures which decreases the load-bearing capacity. Kordina [5] gives a tabular overview of explosive spalling due to hazardous tunnel fires over the last century. The table includes the probable cause of the fires, the number of involved vehicles that burned off and the measured spalling depths. During these fires, thermo-hydraulic and thermomechanical processes are commonly accepted as the two main damaging processes that lead to explosive spalling. Hereinafter, both damage mechanisms are explained for an infinite, unrestrained, and unilateral heated concrete member. Further, these processes are induced by a large temperature gradient due to a low temperature conductivity of the composite material.

1.1 Thermohydraulic damage mechanism

Concrete has different types of bound water. The amount of free and physical bound water depends mainly on the water-cement ratio and the curing conditions. Additionally, water is chemically bound in the cement matrix of the concrete during the hydration process of the cement. In case of fire and an increase of the temperature, the different types of water vaporise and are released at the fire exposed area. The expansion of the steam is hindered by the limited amount of pore space and the continuous vaporisation process leads to high water vapour pressures inside the concrete. Due to the temperature gradient, the water is vaporised only near the fire exposed surface and a pressure gradient forms between the location of the phase transformation and deeper parts of the member. Therefore, a pressure induced steam flow occurs within the capillary pore system [6]. However, in deeper parts of the member the water temperature is beneath the point of vaporisation and the steam condenses. The ongoing steam flow and condensation process form an impermeable, saturated zone in a certain depth. This area is called “moisture clog” [7]. The pore pressure increases in these cooler regions of the member due to the continuous income of steam. As a result, local tensile stresses occur within the pore system. These stresses lead to a formation of cracks in the cement matrix that connect to a capillary pore

system. If these stresses exceed the tensile strength of the concrete, explosive spalling occurs.

1.2 Thermomechanical damage mechanism

The concrete member reacts to the unilateral heating with an expansion of its components. During the heating phase, the cement stone dehydrates and shrinks [8] while the aggregates expand continuously [9]. This discrepancy results in the formation of cracks. With an increasing temperature, the thermal expansion of the concrete member is mainly influenced by the aggregates. Due to the temperature gradient, the expansion of the member decreases with greater distance to the fire exposed surface. The stiffness of the concrete hinders an expansion of the member. This results in an increase of thermal induced compressional stresses parallel to the surface and transverse tensile stresses. Those tensile stresses extend into deeper layers of the member. If the stresses exceed the tensile strength of the concrete, macroscopic cracks form and can result in spalling.

Both damage mechanisms proceed at the same time. Also, the thermomechanical induced cracks enable the thermohydraulic induced steam flow inside the concrete member. It is difficult to separate both mechanisms because measuring instruments inside a specimen affect the initial damaging behaviour. However, the combination of the two mechanisms is generally accepted as the main factors for explosive spalling.

1.3 Size effect

The investigation of the specimen size as an indicating factor for the degree of damage has its origins in fracture mechanics [10]. Ožbolt [11] found that the fracture propagation and the released energy are fundamental parameters to analyse the fracture behaviour of concrete specimens. In fracture mechanics the size effect is described by “type 1” and “type 2” size effects, depending on the tested material and crack size [12]. Primarily investigations on torsional failure of plain and reinforced concrete beams display size effects for three different specimen sizes with a constant length to cross-section ratio of 8/3 [13]. The results show a decrease of the nominal stress at point of failure with an increasing specimen size. However, in concrete spalling the additional thermal stresses



result in even more complex damaging processes that are unique for every tested concrete. A categorised description of the damaging processes and concrete spalling is part of current research. Table 1 shows different publications of single-sided fire tested concrete specimens for one specimen size and comparative multi-scale studies. It is not possible to investigate the size effect by comparing small scale specimens [21, 22], intermediate scale specimens [23, 24] and large members [25] provided by different studies. The spalling of the specimens increases while comparing these studies of small scale specimens [21] and full scale members [25]. However, the usage of different concrete mixtures, fire curves, curing conditions as well as restraints and loadings, prohibit a comparison regarding the effect of the specimen size on the spalling behaviour.

Thus, several research groups investigated the spalling behaviour including size effects, whereas only three displayed publications considered all three specimen sizes (full scale members, intermediate scale slabs, small scale specimens) [14–16]. All these studies show more severe spalling due to an increase of the specimen size for the same concrete mixture. However, the comparability of the spalling depths is limited by varying testing conditions for the different specimen sizes. In the study of Ali et al. [16] four specimen sizes ($3.38 \text{ m} \times 3.38 \text{ m} \times 0.2 \text{ m}$, $1.075 \text{ m} \times 1.075 \text{ m} \times 0.2 \text{ m}$, $1 \text{ m} \times 0.4 \text{ m} \times 0.4 \text{ m}$ and $\varnothing 0.1 \text{ m}$; $h = 0.2 \text{ m}$) including different aggregate sizes were investigated. The large scale and medium scale specimens were tested with a single-side fire exposed surface. The smaller columns and cylinders were set inside the furnace and therefore, fire exposed on more than one side. Additionally, the age of the specimens at the day of the fire tests had a large variance for every specimen type, whereas the maximum difference was 596 d (44 d and 640 d). Thus, the strength properties of the different specimens were too high to compare the

spalling behaviour during the fire tests. The study of Boström et al. [14] is a complex investigation of concrete spalling for four self-compacting concrete mixtures, six tunnel lining mixtures, 9 specimen types from small scale up to full scale. A comparison of the spalling behaviour of each mixture is difficult due to the varying restraints and loading conditions as well as the multi-sided testing of the small scale specimens. Guerrieri et al. [17] investigated the spalling behaviour of a normal strength (28 d compressive strength: 25 MPa) and high strength (28 d compressive strength: 80 MPa) concrete mixture in dependence of different specimen sizes (small scale: $0.3 \text{ m} \times 0.3 \text{ m}$ and full scale: $1.1 \text{ m} \times 1.1 \text{ m}$), different specimen thicknesses (50 mm, 100 mm and 200 mm) without external loading or restraints. The fire exposed area of the specimens was reduced due to the test setup and a cold rim occurred at the border of the specimens. The results show that the specimen size has a large influence on the spalling behaviour. Thus, the spalling volume increases with an increasing specimen size, thickness and compression strength. Unfortunately, the difference of specimen sizes and spalling volumes are too large to interpret and an intermediate scale specimen size is needed to improve the significance to the size effect [17, 18]. The research of Mohaine et al. [15] investigated the spalling behaviour of four different specimen sizes including passive restraints on the small scale specimens to create similar stress conditions compared to the center of a large concrete member. Small cylinders ($\varnothing 0.1 \text{ m}$; $h = 0.22 \text{ m}$), two types of round specimens restrained by a steel ring with sizes of $\varnothing 0.3 \text{ m}$; $h = 0.11 \text{ m}$ and $\varnothing 0.61 \text{ m}$; $h = 0.3 \text{ m}$ as well as members that have a similar size to the full scale member of this paper ($1.7 \text{ m} \times 0.98 \text{ m} \times 0.2 \text{ m}$) were tested. One concrete mixture that was prone to spall during the fire tests was used for all specimens. The full scale specimens were tested unloaded and loaded uniaxial in compression with 0.75 MPa. The results show a spalling depth of 144 mm and 114 mm for the ring restrained specimens ($\varnothing 0.61 \text{ m}$; $h = 0.3 \text{ m}$) while the loaded member had a spalling depth of 105 mm. However, it is assumed that the different placements of the reinforcement and therefore, a smaller covering of the full scale member have a significant influence on the spalling behaviour.

Based on the previous studies, the fire tests presented in this contribution aim on the size effect of six different concrete mixtures and three specimen

Table 1 Overview of different studies for one scale and multi scale spalling tests for single sided fire tests

Specimen size	One scale tests	Multi-scale tests
Full scale members	[25]	[14–19]
Intermediate scale slabs	[23, 24]	[14–16, 19]
Small scale specimens	[21, 22]	[14–18, 20]

sizes under comparable testing conditions. Besides the prior described effects of the multi-scale approaches, the spalling behaviour depends on the concrete composition as well. For instance, the water-cement-ratio, the porosity as well as the permeability, the presence of reinforcement, polypropylene fibres and the type of aggregate can influence the impact of the thermal induced damage [26]. Additionally, external factors, for instance external restraints [15] or loads [19], increase the spalling of a member compared to a concrete that can expand freely.

2 Materials

2.1 Test set-up

To analyse the spalling behaviour of different specimen sizes under comparable conditions, a novel test set-up has been developed (Fig. 1) [27]. This test set-up enables fire tests for a variety of specimen sizes. Full scale slabs, intermediate scale cuboids and small scale cylinders are tested in one furnace. Six intermediate scale and twelve small scale specimens are tested simultaneously. The concrete specimens are mounted to two I-beams using embedded anchor channels and placed in a central position on top of the furnace. Additionally, the remaining openings are enclosed with fire-resistant concrete slabs. All concrete specimens were tested unrestrained and without external loading. Two oil burners are installed on both endings of the furnace to simulate real fire scenarios up to

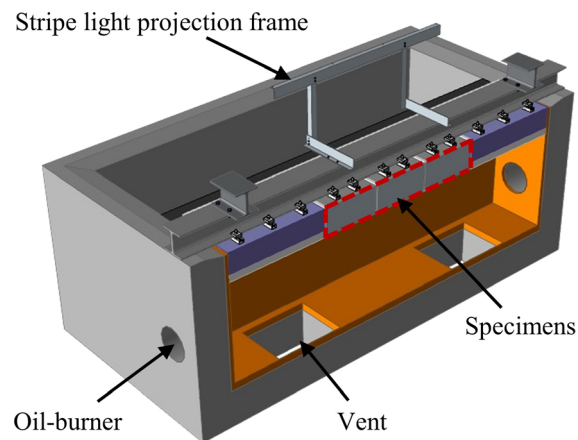


Fig. 1 Overview model of the test set-up including an example for the intermediate scale specimen size [27]



1200 °C for the different concrete mixtures. During this project, two different fire curves were used to carry out the spalling behaviour of two different areas of application. Tunnel lining concrete mixtures were tested with the RABT curve [28], and the construction building concrete mixtures were exposed to the ISO standard fire curve [29].

2.2 Concrete mixtures

Six concrete mixtures were developed to cover a wide range of different applications in civil engineering (Table 2). Two of these concrete mixtures (C1 and C2) are used for tunnel linings. Both concrete mixtures have similar ingredients. In case of C2, polypropylene fibres (PP-fibres) are added to the fresh concrete during the process of mixing. The fibres are a common avoidance strategy for explosive spalling. Their mode of action has already been investigated [30] and Eurocode 2 recommends an addition of at least 2 kg/m³ PP-fibres to the fresh concrete mixture of HPC [31]. Therefore, the comparison of mixture C1 and C2 complements previous studies that investigated the influence of PP-fibres to avoid the occurrence of spalling. The four other mixtures (C3-C6) represent different concretes for several applications. The high strength concrete (HSC, C3) is a mixture that was developed at BAM and its spalling behaviour was already investigated [32]. Due to a low w/c ratio and the high amount of silica fume additives (11% of the cement weight), this mixture is very prone for explosive spalling. Therefore, the expected spalling behaviour of the HSC is perfect to evaluate size effects. The concrete mixture C4 is a self-compacting concrete and a HPC as-well. Hereby, the main difference compared to other concrete mixtures is limestone powder added to the fresh concrete. The mixtures C5 and C6 are similar ordinary concretes and differ only of coarse aggregates. Mixture C5 includes quartzitic gravel and mixture C6 contains basalt. The comparison of both mixtures focusses on the thermo-mechanical influence of different thermal expanding aggregates during the fire test.

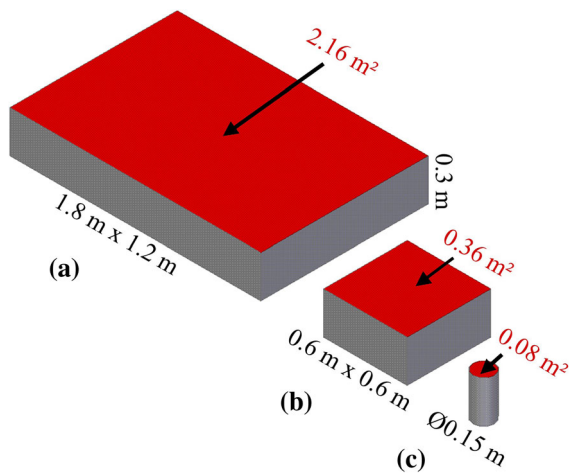
2.3 Specimens

Three different specimen sizes are tested to evaluate a size effect for all six concrete mixtures (Fig. 2). Full

Table 2 Overview of the six concrete mixtures

	Tunnel lining concrete C1	Tunnel lining concrete C2	High strength concrete C3	Self-compacting concrete C4	Ordinary concrete C5	Ordinary concrete C6
Type of material	Amount of components [kg/m ³]					
Cement (CEM I 42.5 R)	320	320	580	300	270	270
Water	160	160	170	180	175	175
Fly ash	80	80	0	0	80	80
Silica fume	0	0	63.8	0	0	0
Limestone powder	0	0	0	301	0	0
Superplastiziser	3.52	11.2	14.5	8.55	2.7	2.7
PP fibres ($\varnothing 19.8 \mu\text{m} \times 6 \text{ mm}$)	0	2	0	0	0	0
Aggregates (quartzitic)						
0/2 mm	675	666	764	668	536	536
2/4 mm	160	158	229	116	285	513*
4/8 mm	231	228	535	116	339	158*
8/16 mm	711	702	0	652	624	711*
28 d Cube compressive strength [MPa]	65	62	104	54	50	56
Fire curve	RABT	RABT	ISO834	ISO834	ISO834	ISO834

*Basaltic gravel

**Fig. 2** Sketches of the **a** full scale specimens, **b** intermediate scale specimens and **c** small scale specimens with the fire exposed areas

scale specimens (FS, 1.8 m \times 1.2 m \times 0.3 m), intermediate scale specimens (IS, 0.6 m \times 0.6 m \times 0.3 m) and cylindrical small scale specimens ($\varnothing 0.15$ m \times 0.3 m) are used to investigate the spalling behaviour. All full scale and intermediate scale concrete

specimens include a steel reinforcing cage of structural steel bars. The diameter of the steel bars is 12 mm, the mesh width is 20 cm for the full scale specimens and 16 cm for the intermediate scale specimens. The concrete covering of the fire exposed surface is 50 mm as well as on the outer sides of the specimens. Due to their size, the small scale specimens are cast without reinforcement. Thermocouples are placed in depths of 5 mm, 50 mm, and 100 mm from the fire exposed surface to evaluate the temperature distribution inside the concrete specimens. For the full scale specimens, thermocouples were distributed on nine positions across the fire exposed surface (see sketch of Fig. 7).

For the specimens of intermediate scale and small scale the thermocouples are placed in the central position. After casting, the full scale specimens remained inside the formwork for one week, while the intermediate scale and small scale specimens were demoulded from the formwork after one day. Afterwards, every specimen was packed in plastic foil and stored in the laboratory for at least 90 days. Two days before the fire test, the specimens were unwrapped and assembled to the supporting I-beams of the test frame.

Six intermediate scale specimens or twelve small scale specimens were composed for simultaneous testing. The small scale specimens were mounted in a slab of fire resistant concrete. All specimens were scanned with a 3D scanning system before and after the fire tests. To ensure the overlay of the 3D scan before and after the fire test, a measuring frame with fixed target points is assembled to the test frame mount (Fig. 1). This provides two aligned 3D surface models to examine the spalling depth and the spalling volume.

3 Results and discussion

3.1 Differential pictures

The fire induced damage of the concrete specimen surfaces is displayed in detail in Figs. 3 and 4 with the results of the 3D scans. The measurements of the fire exposed surface were taken before and after the fire test and show a vertical differential image. For this purpose, the two recorded grids were overlaid with the

help of the stationary target points of the measuring frame. Afterwards, the unidimensional difference between the two grids along the depth of the concrete members was calculated and displayed in a differential image. These calculated differences represent the spalling depth of the fire exposed surface. Additionally, the spalling volume is estimated in relation to the specimen volume before the fire test. After the fire tests, the surfaces of the full scale specimens show a different spalling behaviour for every concrete mixture (Fig. 3). Four of six specimens spalled, whereas the full scale specimen (FS) of mixture C3 was affected the most and the full scale specimens of mixtures C2 and C6 did not spall. Generally, the results of the concrete mixtures C1 and C2 need to be considered separately from the mixtures C3-C6. Due to their fields of application, the fire curve of mixture C1 and C2 was the RABT fire curve. Whereas the ISO 834 fire curve was used for the HSC, the SCC and ordinary concretes (C3-C6). The spalling depth of specimen FS C1 is relative uniform throughout the surface. Almost the whole concrete covering spalled

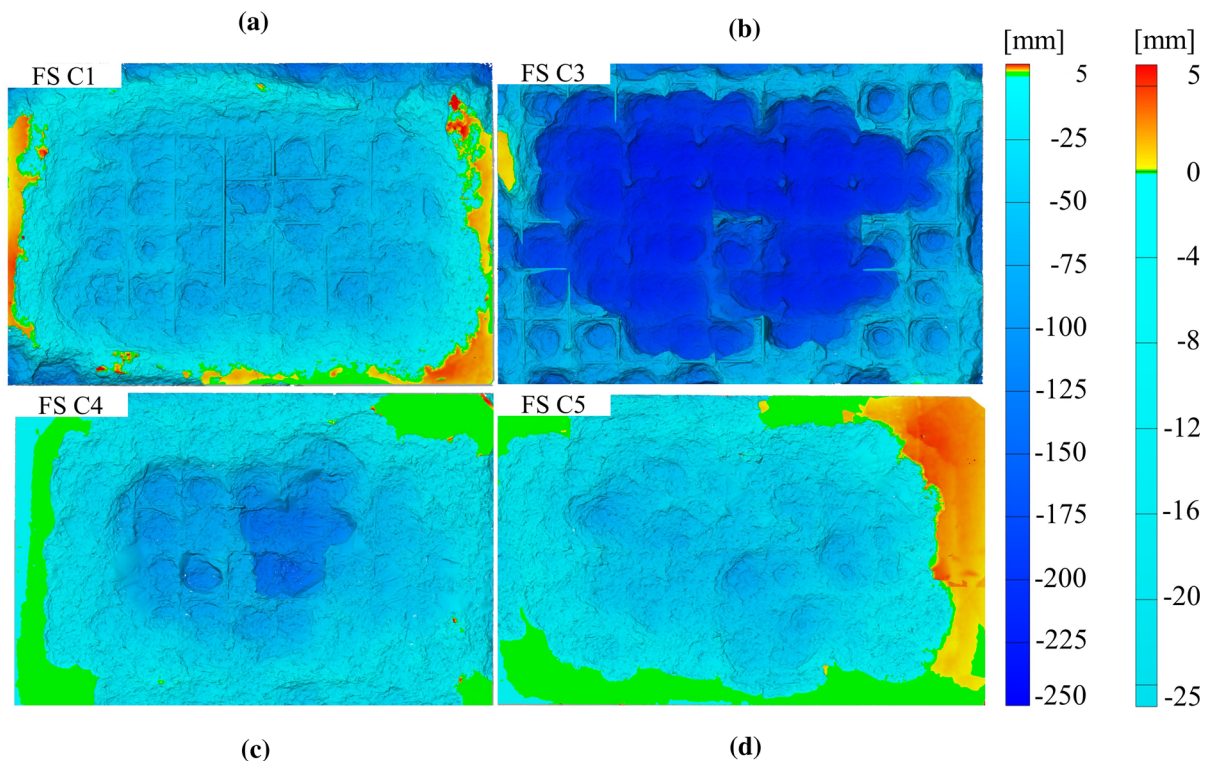


Fig. 3 Results of the 3D scans of the fire exposed concrete surfaces with overlaid colour plots of the spalling depth measured in z-direction for the full scale specimens (Specimens FS C2 and FS C6 did not spall)

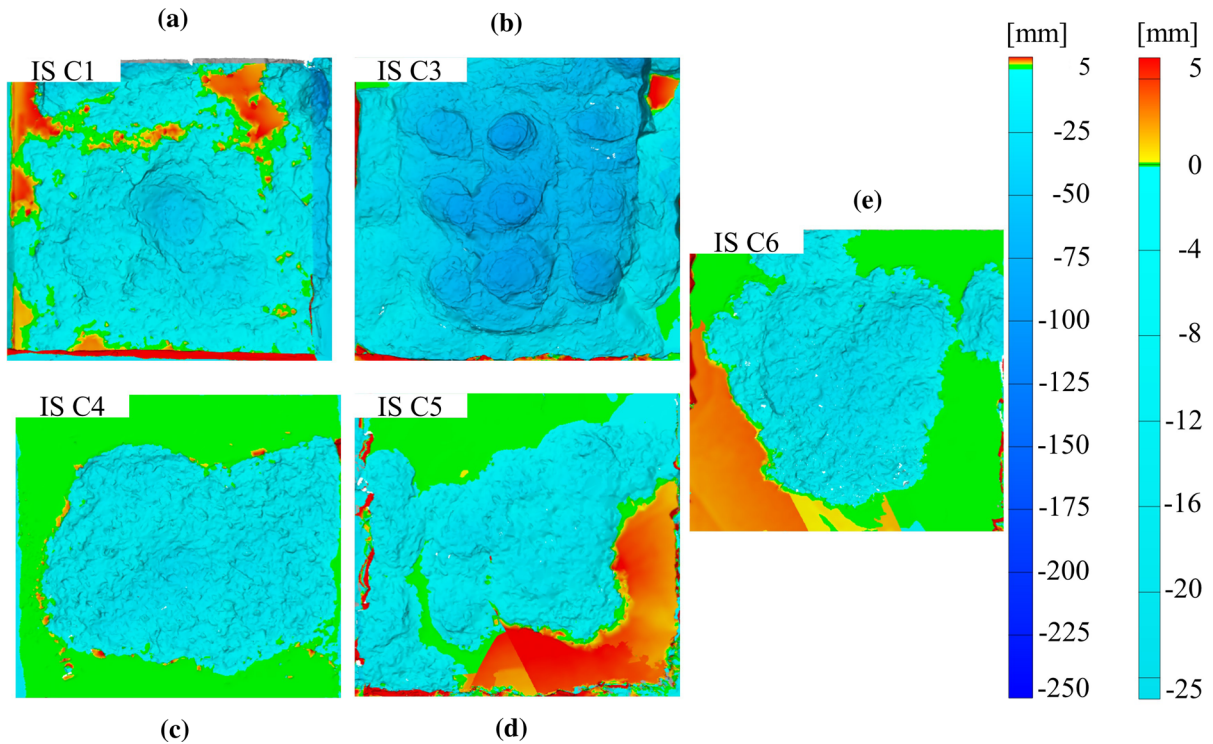


Fig. 4 Results of the 3D scans of the fire exposed concrete surfaces with overlaid colour plots of the spalling depth measured in z-direction for the intermediate scale specimens (IS C2 did not spall)

off and the first reinforcement layer in 0.05 m depth is exposed. The PP-fibres in specimen FS C2 prevent the fire exposed surface from spalling. The fluidised and vaporised PP-fibres build up a system of connected pores and the vaporised water is released through the capillary pores. The thermohydraulic stresses are reduced and the spalling of concrete fragments is prevented. This result underlines the outcome of previous works [24, 30, 33] that PP-fibres have a positive effect on concrete spalling in case of fire. The full scale specimen of mixture C3 shows a complete fire damaged surface with an exposed reinforcement layer. Three-quarter of the specimen thickness spalled off in the centre of the fire exposed area. In this case, the reinforcement prevented a collapse of the concrete slab. The spalled area of FS C4 and FS C5 is pronounced in the centre of the heated area and the spalling depth decreases from the centre to the edge of the fire exposed surface. Thermal induced crack systems that connect deeper parts of the concrete with the surface occur in addition to spalling at the fire exposed surface and on the sides of the specimen. At the edges of the specimen, the vaporised water pours

out through the cracks on two surfaces and the pore pressure reduces compared to the specimen centre. However, the loss of bound water depends on the concrete mixture. The mixtures C1 and C3 are more dense compared to the mixtures C4 and C5. The dense concrete mixtures C1 and C3 reduce the formation of capillar pore systems and thus increase the risk of thermohydraulic induced spalling at the specimens edges. This phenomenon also occurs at the specimen centre. Therefore, the corner and parts of the edge spalled as deep as the centre regarding FS C1 and FS C3 (Fig. 3). On the other hand, the specimens FS C4 and FS C5 have a less dense structure and the results show a reduction of spalling towards the edges. However, for the concrete slab FS C6 no spalling occurred during the fire test. A further discussion on this topic follows in Sect. 3.5. The spalling of the intermediate scale specimens is reduced compared to the full scale specimens (see Figs. 3 and 4). This is an effect of a reduced specimen size that leads to smaller thermomechanical stresses at the surface compared to the full scale specimens. The differential pictures show that the specimen IS C3 is damaged the most

during the fire test and the first reinforcement layer is exposed. The damages at the surface of specimens IS C4, IS C5 and IS C6 are very similar (Fig. 4) and comprise less deep spalling compared to IS C3. Interestingly, the spalled surface area of the intermediate scale specimens appears similar to the full scale specimens of the same mixture. But, the overall thermal damage of the intermediate scale specimens is less and spalling is located around the specimen centre. Contrary to the full scale and intermediate scale specimens, spalling did not occur for the small scale specimens. The fire exposed surface area of the small scale specimens conducts approximately 20 % of the corresponding surface of the intermediate scale specimens. Therefore, the stiffness of the small scale specimens is less compared to the intermediate scale specimens, that leads to more homogeneous expansion. Additionally, thermal induced cracks occur at the fire exposed surface and on the shell surface of the cylinder. The vaporised water pours out of the specimen and thermohydraulic stresses are reduced. All these factors prevent the spalling of the small scale specimens for all concrete mixtures of this test series. Considering all tested specimens, a size effect occurs for four of the six concrete mixtures with a decreasing fire induced damage due to a reduction of the specimen size.

3.2 Spalling depth distribution

The normalised spalling depth distribution are shown in Figs. 5 and 6. This distribution enables a quantitative analysis of the fire induced spalling using the surface plots. For this purpose, a histogram of the spalling depth with a bar width of 5 millimetres was generated. Thereby, the data was normalised by the fire exposed surface and displayed in a diagram. High relative frequencies represent a large area of the specimen that spalled off to this depth. The histograms are a complementation to the differential pictures, especially to examine surface areas with the same spalling depths for each concrete mixture. All plots for the full scale specimens have different distributions. The concrete mixture for tunnel linings (FS C1), the HSC (FS C3) and the ordinary concrete with quartzitic gravel (FS C5) show a peak at the first reinforcement layer around 50 mm depth from the fire exposed surface. Additionally, the mixtures FS C1, FS C4 and FS C5 comprise a peak within 20 mm depth. These

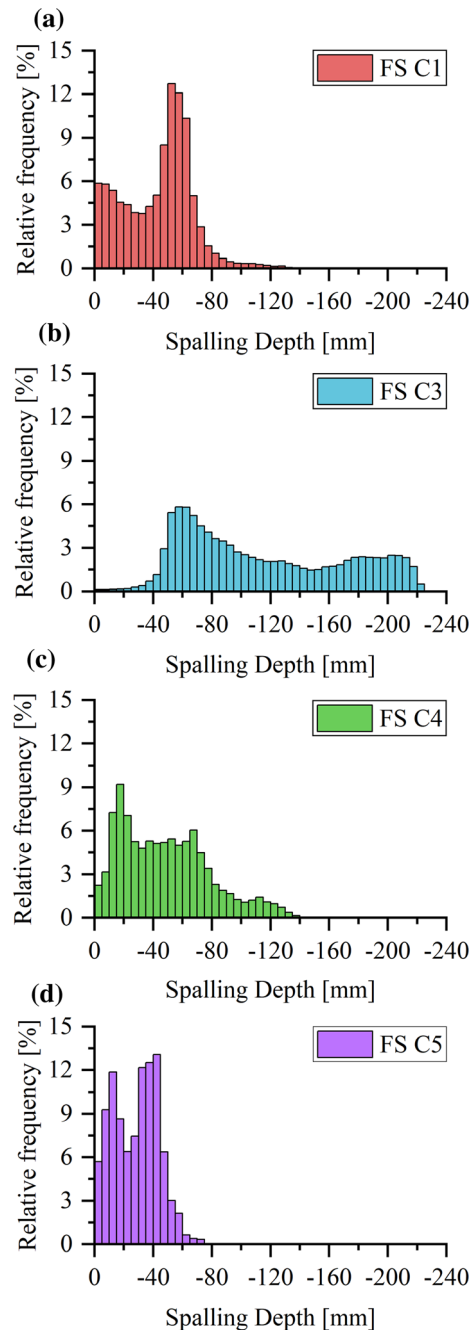


Fig. 5 Normalised spalling depth distribution of the full scale (FS) concrete specimens

high relative frequencies represent large areas that spalled off up to this certain depth. Therefore, FS C1 and FS C5 show a homogeneous spalling behaviour with pronounced peaks in two different depths. After their first peak, the spalling depth distribution of the

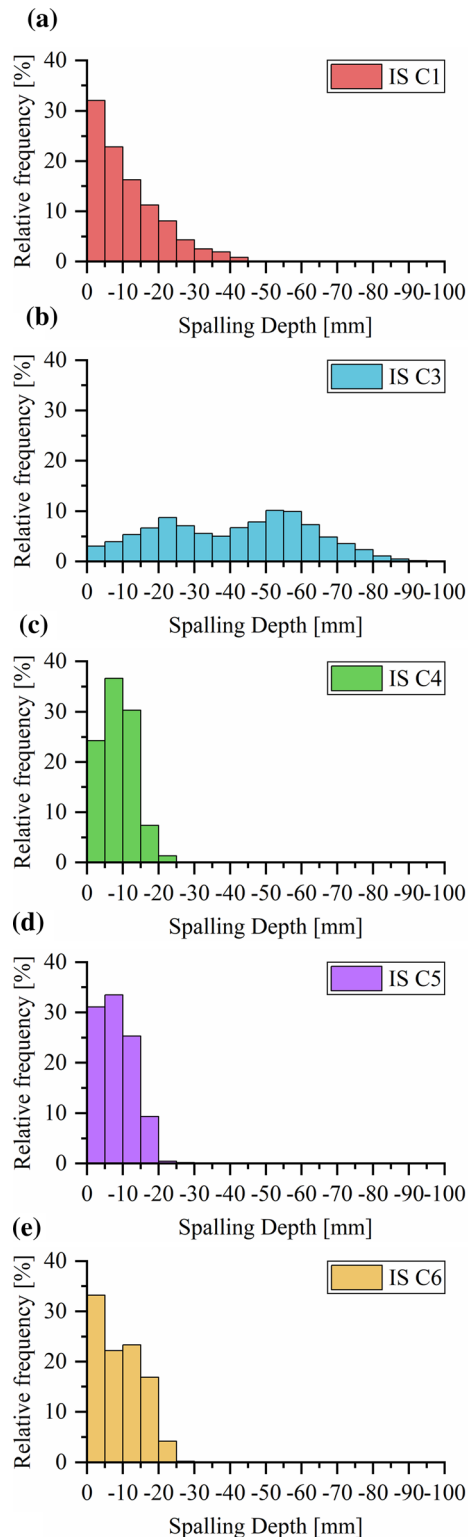


Fig. 6 Comparison of the normalised spalling depth distribution of the intermediate scale (IS) concrete specimens

mixtures FS C3 and FS C4 indicate a funnel-shaped specimen surface with large spalling depths in the specimens centre. The results of the full scale and intermediate scale specimens show that a reduction of the specimen size lead to a shift of the relative frequency values to lower spalling depths. Four of the five displayed mixtures (IS C1, IS C4-C6) show high peaks of relative frequency within the first 15 mm and a strong decrease afterwards. Only the plot of specimen IS C3 comprises spalling beyond the first reinforcement layer and a similar distribution in comparison to the full scale specimens. Therefore, the histograms underline the reduced spalling behaviour of intermediate scale compared to the full scale specimens.

3.3 Spalling volume

The results of the 3D scans provide even more quantitative information. Table 3 shows the absolute spalling volume [dm^3], the spalling volume related to the fire exposed area [$\text{dm}^3 \text{m}^{-2}$], the ratio between spalled and total volume [%] and the maximum spalling depth [mm] of the specimens that are shown in Figs. 3 and 4. The highest spalling volume and maximum spalling depth for the full scale specimens was recorded for the HSC. The second most spalling volume occurred for the SCC followed by the concrete for tunnel-linings and the ordinary concrete with quartzitic gravel. To point out a size effect, it must be considered that the volume of the intermediate scale specimen is six times smaller than the full scale specimen. The results for the concrete mixtures that were affected by spalling in both sizes show that the absolute spalling volume is reduced with decreasing specimen volume. Additionally, the difference of absolute spalling volume within a mixture is at least 2.5 times higher than the difference in specimen volume. However, a size effect is only carried out if at least two different sizes of one mixture are affected by spalling. Due to the usage of PP-fibres, no spalling occurred for mixture C2 for all tested specimen sizes. Additionally, the full scale specimen and small scale specimens of the ordinary concrete with basaltic gravel did not spall. In this scenario, only the intermediate scale specimens spalled. This is further discussed in Sect. 3.5. Considering the other results of the mixtures C1, C3, C4 and C5 spalling is carried out

Table 3 Overview of the spalling depths and volumes for the full scale and one intermediate scale specimen of all concrete mixtures

Specimen	Full scale				Specimen	Intermediate scale			
	Spalling volume			Maximum spalling depth		Spalling volume			Maximum spalling depth
	[dm ³]	[dm ³ /m ²]	[%]			[mm]	[dm ³]	[dm ³ /m ²]	
C1	92.5	42.8	14.3	189	C1	3.5	9.8	3.3	44
C2	–	–	–	–	C2	–	–	–	–
C3	245.8	113.8	37.9	226	C3	13.8	38.3	12.8	93
C4	104.6	48.4	16.1	143	C4	2.5	7.1	2.4	29
C5	55.6	25.8	8.6	76	C5	2.2	6.1	2.0	39
C6	–	–	–	–	C6	1.0	2.7	0.9	34

with two of the three tested specimen sizes. On the other hand, the spalling volume depends on several parameters. These are the specimen size, pore pressure, permeability, the age effect and moisture content, see [2, 34]. Besides the specimen size, the influence of the other factors was not addressed within this study. The results show that a size effect exists but there are too many unknown variables to summarise it with one factor. Additionally, none of the smaller specimens display the same spalling behaviour of the next larger specimen size. Therefore, it can be concluded that the small scale specimens are too small to assess the spalling behaviour of different concrete mixtures. In case of the intermediate scale specimens, further adaptations to the testing conditions must be carried out to achieve results comparable with the full scale specimen. The improvement of the test conditions for the intermediate scale specimens are part of an ongoing research.

3.4 Fire damage propagation

The 3D scans are limited to the surface of the specimens. Thermocouples show the temperature distribution and therefore deliver insight information about the propagation of the thermal damage. Due to the low temperature conductivity, a large temperature gradient forms within the concrete specimens. The loss of concrete covering due to spalling leads to higher temperature in deeper parts of the member. Therefore, the temperature distribution of a concrete specimen is strongly influenced by the spalling behaviour. Figure 7 shows the temperature distribution for the full scale specimen with the highest

spalling volume (FS C3, HSC) and the specimen without spalling (FS C6, OC with basaltic aggregates). Within the first 5 min of the fire test, the temperature distribution at 5 mm from the fire exposed surface is similar for both mixtures (Fig. 7). Afterwards, the temperature of FS C3 increases about 500 K during 10 minutes, whereas the temperature of FS C6 increases about 50 K. Therefore, spalling occurred for FS C3 and at least 5 mm concrete covering spalled off. The resulting concrete covering is reduced for the thermocouples of FS C3 in 50 mm depth and thus, the temperature increases faster compared to the FS C6 with an intact covering. Additionally, both specimens show temperature plateaus at 100 °C for this depth. The liquid water vaporises under normal pressure at this temperature. The vaporisation of the water is an endothermic process and the thermal energy of the surrounding material is used for the phase transition. The duration of the temperature plateau depends on the water volume and energy input for the vaporisation process at the thermocouple in this depth. After a complete vaporisation of the fluid water, the thermal energy leads to an increase of the temperature again. Due to continuous spalling, the temperature plateaus of FS C3 in 50 mm and 100 mm depth from the fire exposed surface occur faster and have a shorter duration compared to FS C6. The plots show the importance of the insulating effect of concrete covering. Further, the temperature increases in larger depths of the concrete in a shorter period of time if the concrete covering spalled off. Previous presented results showed that a reduction of the specimen size lead to reduced spalling for specimens of the same mixture. Figure 8 displays the temperature profiles for

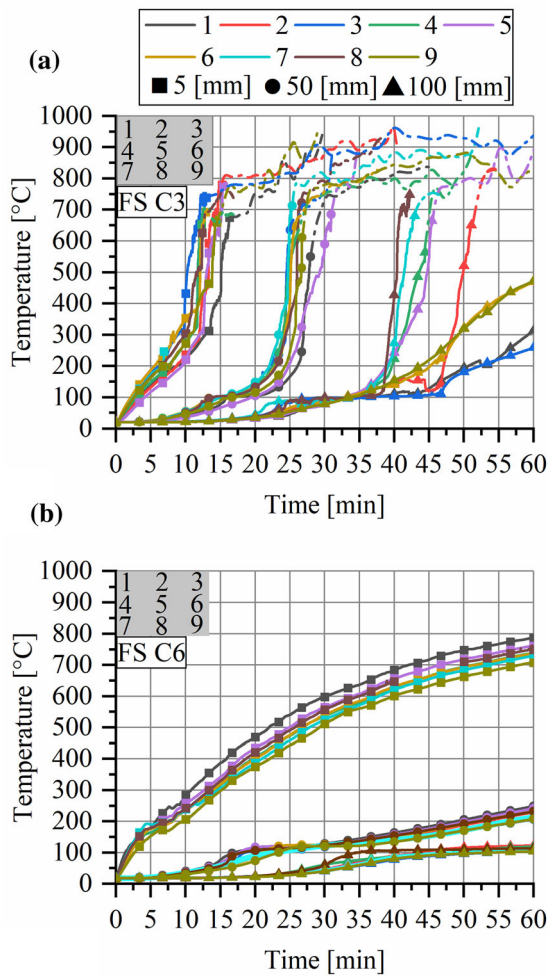


Fig. 7 Temperature profiles of the full scale specimens for **a** the high strength concrete that included spalling and **b** the ordinary concrete with basaltic aggregates without the occurrence of spalling. The diagrams include smoothed temperature distributions for thermocouples without concrete covering

the intermediate scale specimens of the same concrete mixtures as displayed in Fig. 7. The temperature plots of mixture C3 show a similar distribution for the two temperature gauges in 5 mm and 50 mm depth from the fire exposed surface but a smaller temperature increase for the intermediate scale specimen in 100 mm depth. The main difference is that the intermediate scale specimen does not built up a temperature plateau at 100 °C. The smaller fire exposed surface and the cracks at the side of the specimens lead to a faster loss of bound water and a faster temperature increase. This distribution is similar to the thermocouples of the full scale specimen C3 in 100 mm depth at the measuring

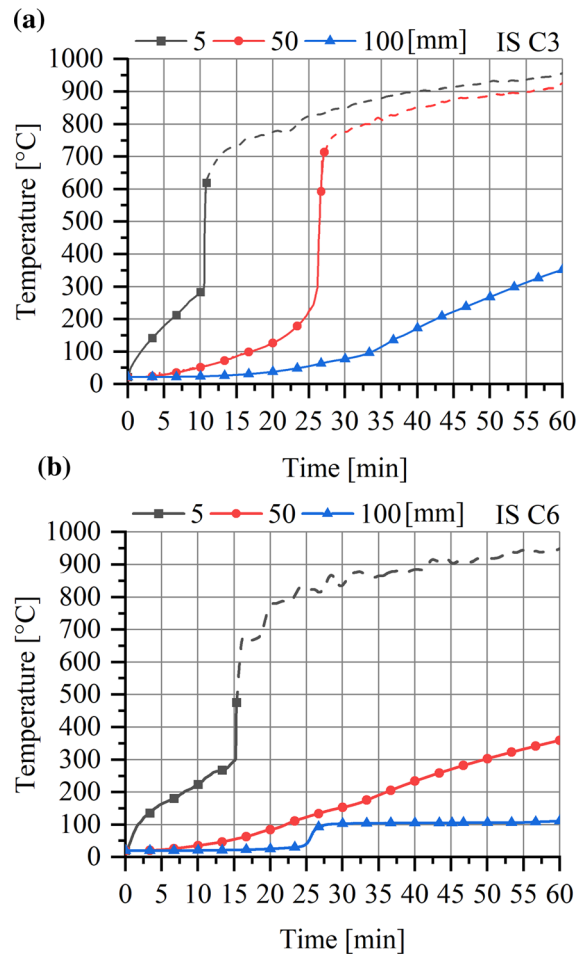


Fig. 8 Temperature profiles of the intermediate scale specimens for **a** the high strength concrete and **b** the ordinary concrete with basaltic aggregates including smoothed temperature distributions for thermocouples without concrete covering

points 6 and 9. Both thermocouples are placed near the specimen side and the loss of bound water lead to a temperature increase without plateau. Another difference is the higher maximum temperature in 100 mm depth of the full scale specimens compared to the one of the intermediate scale specimen in the same depth at the end of the fire test. An increase of the spalling volume leads to higher temperatures for larger specimens and thus, a size effect is also displayed in the temperature diagrams. However, the intermediate scale specimen C6 (IS C6) shows small spalling depths and an intact covering of the reinforcement bars. But, the maximum temperature in 50 mm depth of IS C6 (compare Figs. 7 and 8) is 100 K higher than the corresponding temperature of the full scale

specimen of mixture C6. This shows that even small spalling depths have a marking influence on the temperature penetration insight the test specimens. This in turn leads to higher temperatures of the reinforcing steel and thus to an earlier loss of load bearing capacity.

3.5 An inverted size effect

For four concrete mixtures (C1, C3-C5) a size effect has been displayed within the results of this study. Spalling occurred for the intermediate scale specimens if full scale specimens spalled as well. The only exception is the concrete mixture with basaltic aggregates. Here, the full scale specimen shows a surface with large connected macroscopic cracks and almost no spalling (Fig. 9). Whereas the intermediate scale specimens spalled with a total spalling volume of 1 dm³ each. This result is contrary to the spalling behaviour of the other five concrete mixtures. It is assumed that the curing of the full scale specimen of mixture C6 is different to the intermediate scale specimen due to the inconsistent test results. The condition of a concrete specimen at the day of the fire test depends on several factors. The age of the specimen, the compressive strength at the day of the

fire test and the moisture content due to the storage conditions have an impact on the occurrence of spalling. In this case the storage time and compressive strength of both specimen sizes were similar. The storage conditions were slightly different.

The full scale specimen was demoulded one week after the casting and sealed in plastic foil afterwards. The intermediate scaled specimens were demoulded just one day after casting and subsequently covered with a thin, moist crepe paper to prevent shrinkage cracks and also wrapped in plastic foil. The moisture content was determined with small cylinders (Ø0.1 m × 0.3 m) that were manufactured simultaneously with the fire tested specimens. Those cylinders were demoulded after one day of casting and sealed in plastic bags without further water content and stored next to the large scale specimens. The moisture content was measured on the day of the fire test. The results show a reduced moisture content in the batch of the full scale specimen compared to the intermediate scale specimens. This is a possible factor that spalling did not occur for the specimen FS C6.

4 Conclusions

The mixtures shown in this study present a broad range of applications of concrete in civil engineering. Considering all specimen sizes, five of the six concrete mixtures spalled during the fire tests. The specimen size affects the maximum spalling depth and the spalling volume. The results show that spalling is reduced for the intermediate scale specimens compared to the full scale specimens. None of the small scaled specimens spalled. A reduction of the specimen size and thus a reduced fire exposed surface change the characteristics of the thermal induced damage mechanisms. The ratio of the surface area to the thickness of the specimen decreases from full scale specimens to small scale specimens. Due to the large temperature gradient, a reduced stiffness and the unrestraint test set-up, the expansion of the intermediate scale specimens and small scale specimens lead to lower thermal stresses compared to the full scale specimens. Additionally, macrocracks occur at the fire exposed and the shell surface of the small scale specimens. The vaporised water escapes through the cracks and the thermohydraulic damage is reduced. Further, two similar concrete mixtures for tunnel linings were

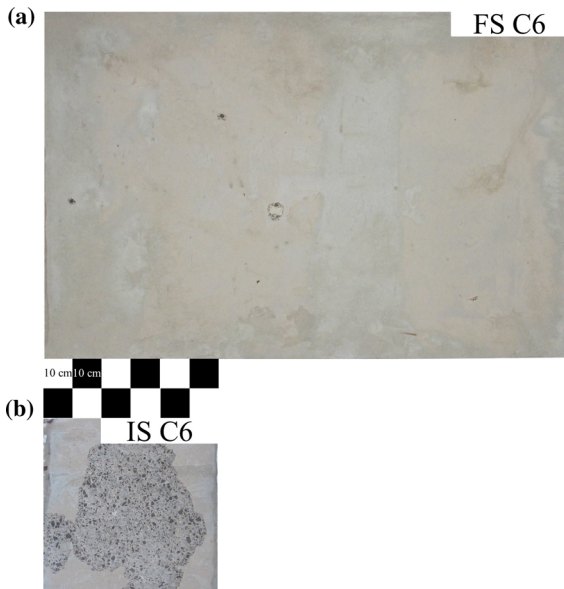


Fig. 9 Displaying the different spalling behaviour of **a** the full scale (FS) and **b** the intermediate scale (IS) concrete specimens of the concrete mixture C6

tested. PP-fibres were added to the fresh concrete for one mixture. As a result, the PP-fibre reinforced concrete did not spall. This underlines the positive influence of the PP-fibre to prevent spalling. All specimens of the mixture without fibres were affected by spalling, while none of the specimens with PP-fibres spalled. The full scale specimen of the ordinary concrete mixture with basaltic aggregates showed no spalling, while the smaller intermediate scale specimen spalled. In this case, a lower moisture content for the larger specimen is a possible explanation for reduced thermohydraulic stresses. The thermal stresses are too low to induce spalling. However, this study shows that size effects exist but more fire tests are needed to identify a measurable factor for the spalling of different specimen sizes. The results display a significant difference in spalling between the full scale and intermediate scale specimens. The test set-up of the intermediate scale specimens must be adjusted to achieve comparable stress conditions between the intermediate scale specimens and the central surface of the full scale specimens. For future investigations a restrained test set-up for the intermediate scale specimens should be implemented to the fire tests to provide a more realistic illustration of larger members. This problem will be addressed in further research.

Acknowledgements The authors gratefully acknowledge the funding of this research by the German Research Foundation (DFG RO 5145/1-1). Further, we gratefully acknowledge the employees of the Division of Fire Engineering, the Division of Building Materials and Division of Technology of Construction Materials at BAM that are part of this study for their support.

Funding Open Access funding enabled and organized by Projekt DEAL. The research leading to these results received funding from the German Research Foundation under Grant Agreement No DFG RO 5145/1-1.

Declarations

Conflict of interest The authors have no relevant financial or non-financial interests to disclose.

Open Access This article is licensed under a Creative Commons Attribution 4.0 International License, which permits use, sharing, adaptation, distribution and reproduction in any medium or format, as long as you give appropriate credit to the original author(s) and the source, provide a link to the Creative Commons licence, and indicate if changes were made. The images or other third party material in this article are included in the article's Creative Commons licence, unless indicated otherwise in a credit line to the material. If material is not included in the article's Creative Commons licence and your

intended use is not permitted by statutory regulation or exceeds the permitted use, you will need to obtain permission directly from the copyright holder. To view a copy of this licence, visit <http://creativecommons.org/licenses/by/4.0/>.

References

- Kirkland CJ (2002) The fire in the channel tunnel. *Tunn Undergr Space Technol* 17(129):132
- Jansson R, Boström L (2013) Factors influencing fire spalling of self compacting concrete. *Mater Struct* 46:1683–1694
- Lo Monte F, Felicetti R, Rossino C (2019) Fire spalling sensitivity of high-performance concrete in heated slabs under biaxial compressive loading. *Mater Struct* 52:14. <https://doi.org/10.1617/s11527-019-1318-0>
- Kalifa P, Menneteau FD, Quenard D (2000) Spalling and pore pressure in HSC at high temperatures. *Cem Concr Res* 30:1915–1927
- Kordina K (2003) Brände in unterirdischen Verkehrsanlagen. *Bautechnik* 80:327–338
- Stelzner L, Powierza B, Tyler O, Dlugosch R, Weise F (2019) Thermally-induced moisture transport in high performance concrete studied by X-ray-CT and ¹H-NMR. *Constr Build Mater* 224:600–609
- Harmathy TZ (1965) Effect of moisture on the fire endurance of building elements. *Am Soc Test Mater Spec Tech Publ* 385:74–95
- Cruz CR, Gillen M (1980) Thermal Expansion of Portland cement paste, mortar and concrete at high temperatures. *Fire Mater* 4:66–70
- Schneider U (1982) Behaviour of concrete at high temperatures. *Deutscher Ausschuss für Stahlbeton* 337
- Bazant ZP, Sener S, Prat PC (1988) Size effect tests of torsional failure of plain and reinforced concrete beams. *Mater Struct* 21:425–430
- Ožbolt J (1995) Maßstabeffekt und Duktilität von Beton- und Stahlbetonkonstruktionen. Universität Stuttgart, Habilitation
- Hoover CG, Bazant ZP (2014) Universal size-shape effect law based on comprehensive concrete fracture tests. *J Eng Mech* 140:473–479. [https://doi.org/10.1061/\(ASCE\)EM.1943-7889.0000627](https://doi.org/10.1061/(ASCE)EM.1943-7889.0000627)
- Bazant ZP (1984) Size effect in blunt fracture: concrete, rock, metal. *J Eng Mech* 110:518–535
- Boström L, Wickström U, Adl-Zarrabi B (2007) Effect of specimen size and loading conditions on spalling of concrete. *Fire Mater* 31:173–186
- Mohaine S, Boström L, Lion M, McNamee R, Robert F (2019) Cross-comparison of screening tests for spalling of concrete. *Fire Mater* 2021:1–14. <https://doi.org/10.1002/fam.2946>
- Mohd Ali AZ, Sanjayan J, Guerrieri M (2018) Specimen size, aggregate size, and aggregate type effect on spalling of concrete in fire. *Fire Mater* 42:59–68
- Guerrieri M, Fragomeni S (2016) Mechanisms of spalling in concrete panels of different geometry in hydrocarbon fire. *J Mater Civ Eng* 12:1–12. [https://doi.org/10.1061/\(ASCE\)MT.1943-5533.0001680](https://doi.org/10.1061/(ASCE)MT.1943-5533.0001680)



18. Pimienta P, Moreau B, Avenel R, Peyrac P, Taillefer N, Larive C, D'Aloia L, Clec'h P (2013) Spalling tests on embedded cores and slabs: a comparative study. MATEC Web conferences 6. <https://doi.org/10.1051/mateconf/20130601003>
19. Lo Monte F, Felicetti R, Meda A, Bortolussi A (2019) Assessment of concrete sensitivity to fire spalling: a multi-scale experimental approach. *Constr Build Mater* 212:476–485
20. Werner S, Rogge A (2015) The effect of various fire-exposed surface dimensions on the spalling of concrete specimens. *Fire Mater* 39:545–556
21. Zhao R, Sanjayan JG (2009) Test method for concrete spalling using small electric furnace. *Fire Mater* 34:189–201. <https://doi.org/10.1002/fam.1020>
22. Hertz KD, Sørensen LS (2005) Test method for spalling of fire exposed concrete. *Fire Saf J* 40:466–476
23. Ozawa M, Tanibe T, Kamata R, Uchida Y, Rokugo K, Parajuli SS (2018) Behavior of ring-restrained high-performance concrete under extreme heating and development of screening tests. *Constr Build Mater* 162:215–228
24. Stelzner L (2021) Analyse des thermisch induzierten Feuchtetransports in gefügedichten Betonen. Dissertation, Universität Stuttgart
25. Dehn F, Werther N, Knitl J (2006) Großbrandversuche für den City-Tunnel Leipzig. *Beton- und Stahlbetonbau* 101(8):631–636. <https://doi.org/10.1002/best.200608186>
26. Hager I, Mróz K, Tracz T (2018) Concrete propensity to fire spalling: testing and observations. MATEC Web of Conferences 163. <https://doi.org/10.1051/mateconf/201816302004>
27. Brecht K, Pistol K, Klemmstein F, Rogge A (2017) Novel test setup for the quantification of the size effect in spalling tests. In: 5th international RILEM workshop on concrete spalling due to fire exposure, Borås, Sweden
28. Zusätzliche Technische Vertragsbedingungen und Richtlinien für Ingenieurbauten ZTV-Ing. Teil 5 Tunnelbau. Bundesamt für Straßenwesen 2014
29. Eurocode 1: Actions on structures - Part 1-2: General actions - Actions on structures exposed to fire; German version EN 1991-1-2:2002, September 2003
30. Pistol K, Weise F, Meng B (2012) Polypropylen-Fasern in Hochleistungsbeton. *Beton- und Stahlbetonbau* 107:476–483
31. Eurocode 2, 1992-1-2: Design of concrete structures-Part 1-2: General rules-Structural fire design, Brussels, Belgium (2004)
32. Huismann S (2010) Materialverhalten von hochfestem Beton unter thermomechanischer Beanspruchung. Dissertation, Technische Universität Wien, Vienna Austria
33. McNamee R, Sjöström J, Biström L (2021) Reduction of fire spalling of concrete with small doses of polypropylene fibres. *Fire Mater* 2021:1–9. <https://doi.org/10.1002/fam.3005>
34. Mindeguia J-C, Pimienta P, Carré H, La Borderie C (2013) Experimental analysis of concrete spalling due to fire exposure. *Eur J Environ Civ Eng* 6:453–466

Publisher's Note Springer Nature remains neutral with regard to jurisdictional claims in published maps and institutional affiliations.

